Photochemical Reactions between C_{60} and Aromatic Thiols. Protonation of C_{60} via Photoinduced Electron Transfer

Maksudul M. Alam,[†] Masahiro Sato,[†] Akira Watanabe,[†] Takeshi Akasaka,[‡] and Osamu Ito*,[†]

Institute for Chemical Reaction Science, Tohoku University, Katahira, Sendai 980-8577, Japan, and Graduate School of Science and Technology, Niigata University, Niigata 950-21, Japan

Received: March 10, 1998; In Final Form: July 8, 1998

Photochemical reactions between C_{60} and aromatic thiols via electron transfer from aromatic thiols to the excited triplet state of C_{60} ($^3C_{60}$*) have been studied by means of laser flash photolysis. In polar benzonitrile, accompanied by the decay of $^3C_{60}$*, the rise of the anion radical of C_{60} ($C_{60}^{\bullet-}$) was observed for thiols, phenols, and disulfides with NH_2 substituents. In the case of aminobenzene disulfide, the cation radical was observed at the same time as $C_{60}^{\bullet-}$, which decayed by back electron transfer. For aminobenzenethiols, the free thio radical was observed, indicating fast deprotonation of the cation radicals of thiols. By the repeated laser-pulse irradiation of C_{60} in the presence of the aminobenzenethiols, the characteristic absorption bands of the monoadduct with C_{60} were observed, suggesting that the monoadduct is formed via electron transfer followed by consecutive radical coupling and protonation reactions. The rate constant of protonation of $C_{60}^{\bullet-}$ was also determined, which supports the proposed reaction mechanism.

Introduction

Extensive studies have revealed that photoexcited fullerenes such as C_{60} act as good electron acceptors in the presence of electron donors.[1−9] The photoinduced electron-transfer reactions of C_{60} have been successfully investigated by photochemical techniques such as laser flash photolysis equipped with near-IR detectors.[2−6,9−11] When concentrations of the donors were not high enough to form appreciable charge-transfer complexes with C_{60} the radical anion of C_{60} ($C_{60}^{\bullet-}$) was usually produced via the triplet state of C_{60} ($^3C_{60}$*) in polar solutions.[2,5,9,10] For these studies, various aromatic amines and alkylamines were predominantly used as electron donors, in accord with the Rehm−Weller relationship.[2,3a,4,5] Recently, we reported that sulfur compounds with high electron-donor abilities such as tetrathiafulvalene (TTF) exhibit photoinduced electron transfer in polar solvents to $^3C_{60}$*, forming stable ion radicals.[10−14] It would be expected that aromatic thiols with electron-donating substituents such as amino and methoxy groups would also transfer an electron to $^3C_{60}$* forming ion radicals, from which adducts might be produced.

In the present study, we measured the transient absorption spectra in the visible and near-IR regions to confirm the photoinduced electron transfer between C_{60} and the aromatic thiols, phenols, and disulfides (Scheme 1) and the consequent adduct formation. The reaction mechanism of photoadduct formation between C_{60} and aromatic thiols was elucidated by combining the steady-state absorption measurements. In these reactions, a prominent solvent effect on the rate and yield of adduct formation was found.

Experimental Section

Materials. C_{60} was obtained from Texas Fullerenes Corporation in a purity of 99.9%. Commercially available benzenethiols, phenols, and benzene disulfides were used after purification by recrystallization. High purity tetrathiafulvalene (TTF) and trifluoroacetic acid were purchased from Aldrich Chemical (USA) and Merck-Schuchardt (Germany), respectively. Benzonitrile, benzene, and *o*-dichlorobenzene used as solvents were of HPLC grade and spectrophotometric grade.

SCHEME 1

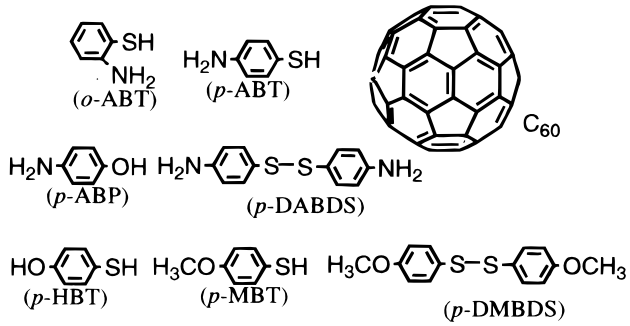

Transient Absorption Measurements. The nanosecond laser photolysis apparatus was a standard design with a Nd:YAG laser (6 ns fwhm).[15] The C_{60} solution was photolyzed with SHG light (532 nm), and the time profiles were followed with a photomultiplier tube (PMT) in the visible region. For transient absorption measurements in the near-IR region, a germanium avalanche photodiode module (Ge-APD; Hamamatsu) attached to a monochromator was employed as a detector to monitor the probe light from a pulsed Xe lamp (60 μs fwhm). The details of the experimental setup are described elsewhere.[16]

The sample solutions were deaerated by bubbling with Ar gas for 15 min before measurements. The laser photolysis was performed with the solution in a rectangular quartz cell with a 10 mm optical path. All the measurements were carried out at 23 °C.

Absorption spectra of the radical cations of sulfur compounds were measured by γ-irradiation in frozen glassy butyl chloride solution at 77 K.

[†] Tohoku University.
[‡] Niigata University.

S1089-5639(98)01440-6 CCC: $15.00
Published on Web 09/02/1998

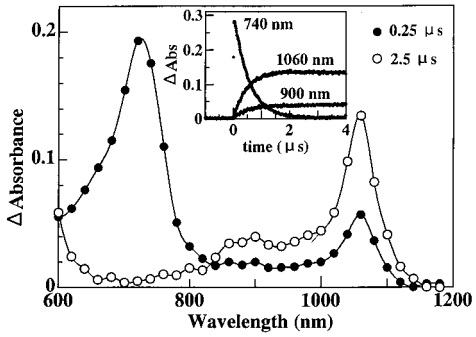

Figure 1. Transient absorption spectra observed after laser photolysis of C_{60} (0.1 mM) in the presence of *p*-ABT (0.8 mM) with 532 nm light in the visible and near-IR regions in Ar-saturated benzonitrile; Ge-APD was used as a detector. Insert shows time profiles of absorption bands.

The mass spectra of the adducts were measured by the fast atom bombardment method. The IR spectra of the adducts were measured after separation of the adducts with TLC.

MO Calculations. Ionization potentials and dipole moments of thiols were calculated by MNDO using the programs incorporated in MOPAC.[17]

Results and Discussion

Steady-State Absorption. C_{60} absorbs light in the UV−visible region, showing a broad absorption band in the region of 400−650 nm,[10] which allows one to excite C_{60} with laser light at 532 nm because of the lack of the absorption of many electron donors in this region. When these donors were mixed with C_{60}, no specific change of the absorption bands was observed in benzonitrile and benzene solutions under the concentration range (0.05−3.0 mM) used for transient absorption and product formation experiments. Thus, specific interaction between donors and C_{60} was not observed in the ground state.

Transient Absorption Spectra. The transient absorption spectra in the visible and near-IR regions observed by laser photolysis of C_{60} (0.1 mM) with 532 nm light in the presence of *p*-aminobenzenethiol (*p*-ABT) (0.8 mM) in Ar-saturated benzonitrile are shown in Figure 1. A sharp absorption peak at 740 nm, appearing immediately after nanosecond laser exposure, is attributed to the triplet−triplet absorption band of $^3C_{60}$*.[9,10,18−26] The decay of $^3C_{60}$* was accelerated in the presence of *p*-ABT. After the decay of $^3C_{60}$*, a new absorption band appeared at 1060 nm with a shoulder at 920 nm, assigned to $C_{60}^{\bullet-}$.[1,4,9,10,22−25]

In benzene, the decay of $^3C_{60}$* was not accelerated compared with that in the absence of *p*-ABT. Thus, deactivation induced by *p*-ABT, including electron transfer, does not take place in nonpolar benzene. For other donors in Scheme 1, no increase in decay of $^3C_{60}$* was observed in benzene.

In benzonitrile, similar transient absorption spectra showing the formation of $C_{60}^{\bullet-}$ were observed for the thiols, phenols, and disulfides with an NH_2 group, such as *o*-aminobenzenethiol (*o*-ABT), *p*-aminobenzenephenol (*p*-ABP), and *p*-diaminobenzenedisulfide (*p*-DABDS) while electron transfer does not take place for other derivatives with methoxy and hydroxy groups, such as *p*-methoxybenzenethiol (*p*-MBT), *p*-hydroxybenzenethiol (*p*-HBT), and *p*-dimethoxybenzenedisulfide (*p*-DMBDS). These findings suggest that the electron-donating ability of the methoxy and hydroxy groups is not strong enough compared to that of the amino group for electron transfer to $^3C_{60}$*.

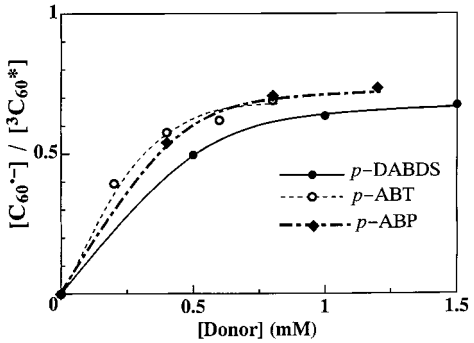

Figure 2. Plots of efficiency of $C_{60}^{\bullet-}$ formation $\{[C_{60}^{\bullet-}]/[^3C_{60}^*]\}$ vs [donor] in Ar-saturated benzonitrile.

TABLE 1: Rate Constants for Forward Electron Transfer (k_{et}) Calculated from Quantum Yields (Φ_{et}), Observed Second-Order Rate Constants (k_2) in Benzonitrile and Rate Constants for Decay of $C_{60}^{\bullet-}$ (k_{decay}^A)[a]

donors	IE[b] (eV)	k_2[c] ($M^{-1}\,s^{-1}$)	Φ_{et}[d]	k_{et}[e] ($M^{-1}\,s^{-1}$)	k_{decay}^A/ϵ_A[f] (cm s^{-1})	k_{decay}^A ($M^{-1}\,s^{-1}$)
p-ABT	10.61	2.3×10^9	0.68	1.4×10^9	2.8×10^5	3.3×10^9 [g]
o-ABT	10.96	5.9×10^7	0.75	4.4×10^7	2.9×10^5	3.6×10^9 [g]
p-ABP	11.08	2.6×10^9	0.72	1.9×10^9	5.0×10^5	6.1×10^9 [h]
p-DABDS	7.71	2.6×10^9	0.66	1.7×10^9	7.2×10^5	8.7×10^9 [h]

[a] Estimation error = ±5% for the values of k_2, k_{et}, and k_{decay}^A. [b] IE represents ionization energy calculated by MO method,[17] for other compounds in Scheme 1: 11.37 eV for *p*-HBT, 11.28 eV for *p*-MBT, and 10.96 eV for *p*-DMBDS. [c] k_2 represents the second-order rate constant obtained from the decay of $^3C_{60}$* at 740 nm. [d] $\Phi_{et} = [C_{60}^{\bullet-}]_{max}/[^3C_{60}^*]_{max}$ was calculated using the observed absorbance and reported ϵ values (ϵ of $^3C_{60}$* at 740 nm, 16 100 $M^{-1}\,cm^{-1}$ ϵ of $C_{60}^{\bullet-}$ at 1060 nm, 12 100 $M^{-1}\,cm^{-1}$).[9,10,26,28] [e] k_{et} represents the forward electron-transfer rate constant obtained from $\Phi_{et}k_2$. [f] ϵ_A= 12 100 $M^{-1}\,cm^{-1}$ at 1060 nm.[9,10,28] [g] k_{rc}. [h] k_{bet}.

Kinetics and Quantum Yield of Electron Transfer. The decay rate of $^3C_{60}$* at 740 nm seems to be in good agreement with the rise rate of $C_{60}^{\bullet-}$ at 1060 nm, as shown in the inserted time profiles in Figure 1. Therefore, electron transfer takes place via $^3C_{60}$*. Since we can observe $^3C_{60}$* and $C_{60}^{\bullet-}$ in the same time frame, the efficiency of $C_{60}^{\bullet-}$ formation via $^3C_{60}$* could be calculated from the absorbance (A_A refers to maximum absorbance of $C_{60}^{\bullet-}$ and A_T to initial absorbance of $^3C_{60}$*) and extinction coefficients (ϵ_A refers to that of $C_{60}^{\bullet-}$ and ϵ_T to that of $^3C_{60}$*) as follows (eq 1):[10,11,27]

$$[C_{60}^{\bullet-}]_{max}/[^3C_{60}^*]_{max} = (A_A/\epsilon_A)/(A_T/\epsilon_T) \qquad (1)$$

Upon substitution of the reported values for ϵ_T and ϵ_A,[9,10,26,28] $[C_{60}^{\bullet-}]_{max}/[^3C_{60}^*]_{max}$ values were evaluated. $[C_{60}^{\bullet-}]_{max}/[^3C_{60}^*]_{max}$ is plotted against [donor] as shown in Figure 2. $[C_{60}^{\bullet-}]_{max}/[^3C_{60}^*]_{max}$ values increase with [donor] and reach a plateau, yielding the quantum yield (Φ_{et}).[10,11,27] The Φ_{et} values are summarized in Table 1. All reaction systems in Table 1 show Φ_{et} in the range of 0.66−0.75. This implies that all of the $^3C_{60}$* was not always converted to $C_{60}^{\bullet-}$; thus, some deactivation processes such as charge-transfer interaction may take place concomitantly with the electron-transfer process in polar solvents. Thus, the electron-transfer mechanism in polar solvents is described as shown in Scheme 2, in which D refers to electron donors (k_{da} and Φ_{da} are the rate constant and quantum yield of the deactivation processes, respectively).

Each decay curve of $^3C_{60}$* at 740 nm obeys first-order kinetics giving a linear relationship between ln(abs) and time. The slope yields the first-order rate constants (k_{obs}), which are in good agreement with the corresponding first-order rate constant

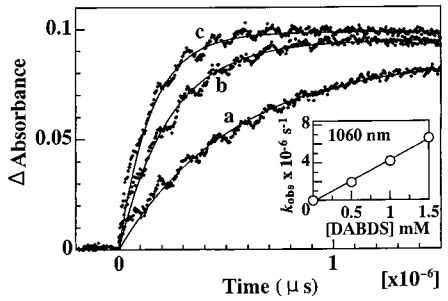

Figure 3. Rise time profiles of $C_{60}^{\bullet-}$ at 1060 nm obtained by 532 nm laser photolysis of C_{60} (0.1 mM) with *p*-DABDS in Ar-saturated benzonitrile; [*p*-DABDS] 0.5 (a), 1.0 (b), and 1.5 mM (c). Insert shows pseudo-first-order plot.

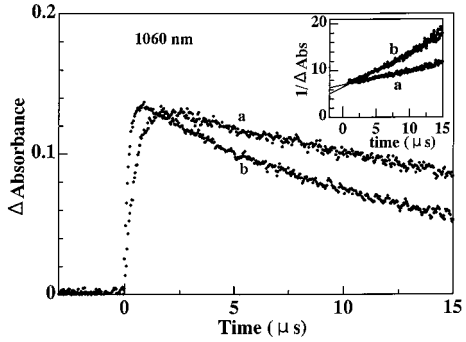

Figure 4. Absorption vs time profiles for decay of $C_{60}^{\bullet-}$ at 1060 nm with (a) *p*-ABT and (b) *p*-DABDS obtained by 532 nm laser photolysis in Ar-saturated benzonitrile. Insert shows Second-order plots.

SCHEME 2

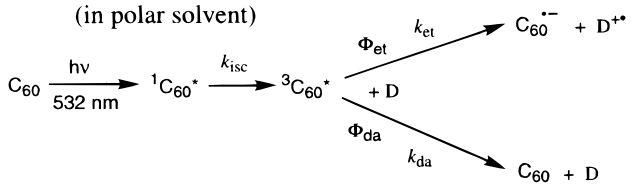

evaluated from curve fitting with a single exponential (Figure 3) for the rise curves of $C_{60}^{\bullet-}$. These k_{obs} values increase with [D]. The pseudo-first-order plot of k_{obs} vs [D] gives the second-order rate constant (k_2) for $^3C_{60}$* with D in benzonitrile (inset in Figure 3). They are listed in Table 1. The rate constants (k_{et}) for electron transfer via $^3C_{60}$* can be finally evaluated by the relation $k_{et} = \Phi_{et}k_2$. These k_{et} values are added to Table 1. From the ionization energies (IE) evaluated from MO calculations,[17] it was found that the derivatives with low IE tend to donate an electron to $^3C_{60}$*. However, IE is not only the criterion, because *p*-ABP shows electron transfer irrespective of its slightly higher IE; rather, the amino substitution is a strong criterion for electron transfer. For *p*-ABT, *p*-ABP, and *p*-DABDS, the k_{et} values are about 1×10^9 M^{-1} s^{-1}, which is only slightly smaller than the diffusion controlled limit in benzonitrile ($k_{diff} = 5.2 \times 10^9$ M^{-1} s^{-1}).[10,11] On the other hand, the k_{et} value for *o*-ABT is smaller than those of the others by a factor of $^1/_{30}$−$^1/_{50}$, although the value of Φ_{et} for *o*-ABT is almost the same as those for the other donors. The main difference between *p*-ABT and *o*-ABT is in their dipole moments, 2.76 D for *p*-ABT and 0.54 D for *o*-ABT. Since the electron transfer takes place only in polar solvents, the dipole moment may be one of the factors determining the k_{et} value.

Back Electron Transfer. After reaching a maximum, $C_{60}^{\bullet-}$ begins to decay as shown in Figure 4, which is illustrated in the long-time scale-up to 15 μs. The decay of $C_{60}^{\bullet-}$ follows

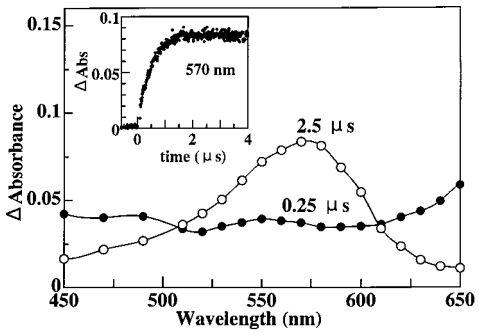

Figure 5. Transient absorption spectra in the visible region observed after laser photolysis of C_{60} (0.1 mM) in the presence of *p*-ABT (0.8 mM) with 532 nm light in Ar-saturated benzonitrile; PMT was used as a detector. Insert shows time profile of absorption band at 570 nm.

SCHEME 3

For stable cation radicals

$$C_{60}^{\bullet-} + D^{\bullet+} \xrightarrow{k_{bet}} C_{60} + D$$

For unstable cation radicals of thiols

$$ArSH^{\bullet+} \xrightarrow{k_{dp}} ArS^{\bullet} + H^{+}$$

$$C_{60}^{\bullet-} + ArS^{\bullet} \xrightarrow{k_{rc}} {}^{-}C_{60}\text{-}SAr$$

second-order kinetics in polar benzonitrile as shown in the inset to Figure 4 (the observed second-order rate constants are denoted as k_{decay}^{A}).

The slope of the second-order plot yields k_{decay}^{A}/ϵ_A. Upon substitution of the reported values for ϵ_A,[9,10,28] one can obtain the k_{decay}^{A} values, which are also listed in Table 1. Second-order kinetics indicate that $C_{60}^{\bullet-}$ and $D^{\bullet+}$ recombine (Scheme 3) after being solvated as free ions.[9,24,29] Compared with the k_{decay}^{A} values for disulfide and phenol that result from back electron transfer (k_{bet}), the k_{decay}^{A} values observed for *p*-ABT and *o*-ABT are slightly smaller, probably due to radical−radical anion coupling (k_{rc}) after deprotonation (k_{dp}) because the k_{bet} values between the oppositely charged ion radicals may be larger than the k_{rc} values. Although the k_{rc} value for *o*-ABT would be anticipated to be smaller than that for *p*-ABT, for steric reasons, they are found to be similar, probably because of the round surface of C_{60}.

Reactions after Electron Transfer. The transient absorption spectra in the visible region observed by laser excitation of C_{60} with light at 532 nm in the presence of *p*-ABT in Ar-saturated benzonitrile are shown in Figure 5. Immediately after the laser pulse, the tail of the absorption of $^3C_{60}$* was observed in the region of 400−600 nm. With the decay of $^3C_{60}$*, an intense new absorption band appears at 570 nm, which can be attributed to the *p*-aminobenzenethio radical (*p*-$H_2NC_6H_4S^{\bullet}$) in benzonitrile,[30,31] but not to the cation radical of *p*-$H_2NC_6H_4SH$ (*p*-$H_2NC_6H_4SH^{\bullet+}$), since the weak broad absorption band in the region of 400−600 nm characteristic of *p*-$H_2NC_6H_4SH^{\bullet+}$ was observed upon γ-irradiation of *p*-$H_2NC_6H_4SH$ in frozen glassy butyl chloride at 77 K. This supports the deprotonation of *p*-$H_2NC_6H_4SH^{\bullet+}$ to give *p*-$H_2NC_6H_4S^{\bullet}$. The time profile of *p*-$H_2NC_6H_4S^{\bullet}$ at 570 in the inset of Figure 5 indicates that the deprotonation of the thiol hydrogen of *p*-$H_2NC_6H_4SH^{+\bullet}$ takes place quite fast (Scheme 3).

In the case of *p*-aminophenol, no clear transient absorption band due to the *p*-aminophenoxy radical was observed in the region of 400−600 nm, indicating that the deprotonation of

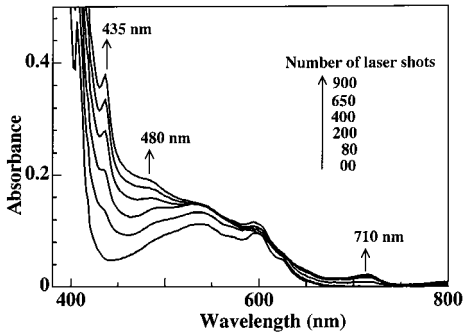

Figure 6. Steady absorption spectral changes observed after 532 nm laser irradiation of C_{60} (0.1 mM) with *o*-ABT (2.0 mM) in Ar-saturated benzonitrile.

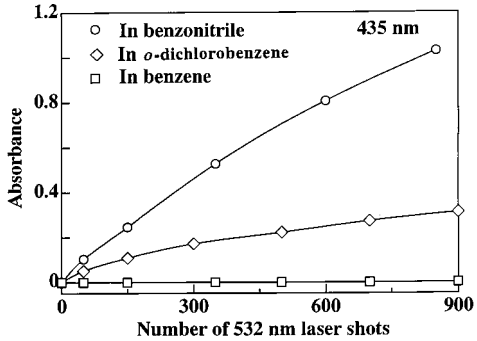

Figure 7. Plots of steady absorption changes at 435 nm vs number of 532 nm laser shots in Ar-saturated solutions for *p*-ABT.

p-$H_2NC_6H_4OH^{\bullet+}$ does not take place. For *p*-DABDS in benzonitrile, only a weak and broad absorption band due to p-$DABDS^{\bullet+}$ was observed in the region of 400−600 nm, which was confirmed by observing a similar absorption band during γ-irradiation of *p*-DABDS. The disproportionation reaction of p-$DABDS^{\bullet+}$ to p-$H_2NC_6H_4S^{\bullet}$ and p-$H_2NC_6H_4S^{+}$ was not observed, based on the absence of the intense absorption band of p-$H_2NC_6H_4S^{\bullet}$ at 570 nm. This is ascribed to the stability of three-electron bonds in p-$DABDS^{\bullet+}$ proposed by Asmus et al.[32] The k_{dp} value of $H_2NC_6H_4SH^{+\bullet}$ is greater than or equal to 10^6 s^{-1}, since the formation of $NH_2C_6H_4S^{\bullet}$ may occur as soon as electron transfer takes place (inset in Figure 5). The protonation reaction may not be so fast as to disturb the second-order kinetics (Figure 4), because of the low concentration of H^+, which is the same as that of $C_{60}^{\bullet-}$ and $NH_2C_6H_4S^{\bullet}$ (ca. 10^{-6} M as calculated from A_A and ϵ_A).

Steady-Light Photolysis. After repeated laser pulse irradiation at 532 nm, which predominantly excites C_{60}, steady-state UV−visible spectra were measured, as shown in Figure 6 for the mixture of C_{60} and *o*-ABT in Ar-saturated benzonitrile. The sharp absorption peak at 435 nm together with a broad band in the region of 450−550 nm and a weak band at 710 nm is characteristic of monoadducts of C_{60}.[29,33,34] Although in benzene no reaction was observed, a slow increase in the absorption bands due to the monoadduct was observed in slightly polar *o*-dichlorobenzene, in which slow photoinduced electron transfer was observed from transient absorption measurements ($k_{et} = 4.0 \times 10^7$ $M^{-1}s^{-1}$ for *p*-ABT) with low Φ_{et} (0.18).

Similar spectral changes indicating monoadduct formation were observed for the mixture of C_{60} and *p*-ABT in Ar-saturated benzonitrile and in *o*-dichlorobenzene, while no appreciable spectral change was observed for other reaction systems, such as *p*-DABDS, *p*-ABP, *p*-MBT, *p*-HBT and *p*-DMBDS. These observations indicate that an H_2N-substituted SH group is responsible for the photoadduct formation with C_{60} in polar solvents. Although an NH_2 group is present in the benzenethiols, phenol, and benzene disulfide with which the electron-transfer reactions occurred, proton transfer was observed only for aminobenzenethiols in polar solvents. Thus, it appears that the proton-transfer process is occurring from the SH, not the NH_2, group. The NH_2 group enhances the electron-donating ability of the phenylthiol and phenol moieties. The rate of the photoadduct formation and its yield vary with changes in the solvent polarity from benzonitrile to benzene. The efficiency of the photoadduct formation in polar benzonitrile is 3 times greater than that in less polar *o*-dichlorobenzene and is zero in a nonpolar solvent such as benzene as shown in Figure 7. This is consistent with the variations in quantum yields of photoinduced electron transfer ($\Phi_{et} = 0.68$, 0.18, and 0.0 in benzonitrile, *o*-dichlorobenzene, and benzene, respectively, for *p*-ABT). These observations suggest that photoinduced electron transfer is the indispensable step for photoadduct formation and also that the higher the electron-transfer quantum yield (Φ_{et}), the higher is the photoadduct formation of C_{60} with ABT.

Presumed Reaction Mechanism. The mass spectrum of the final product separated from *p*-ABT (or *o*-ABT) by TLC shows $m/e = 721$ and 124, which correspond to $H-C_{60}^{\bullet}$ and $^{\bullet}SC_6H_4NH_2$, respectively. The photoadduct is apparently $H-C_{60}-SC_6H_4NH_2$ ($m/e = 845$), but the molecular ion of $m/e = 845$ was not observed because the C−S bond might be easily broken during the FAB-mass spectroscopic measurement. The FT-IR spectra of the isolated sample showed characteristic bands for the amino group in the region of 3000−3400 cm^{-1}. Thus, the

SCHEME 4

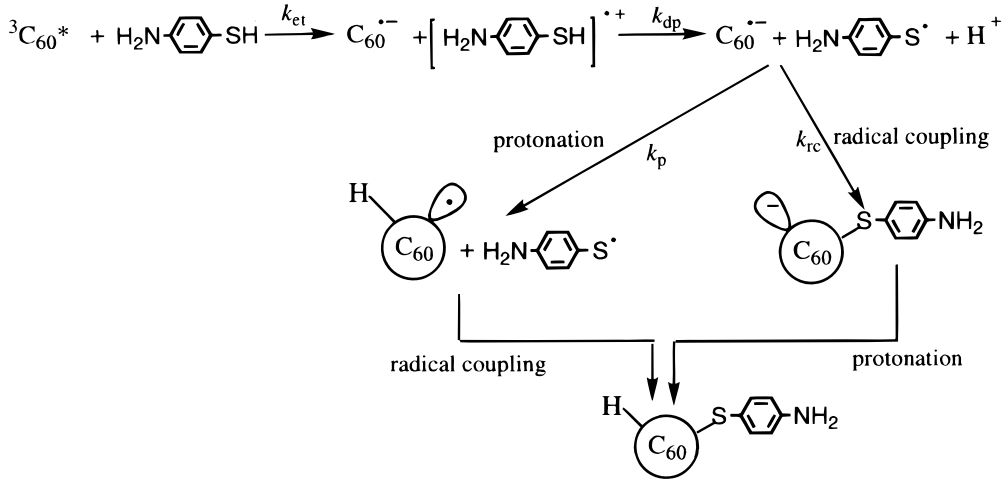

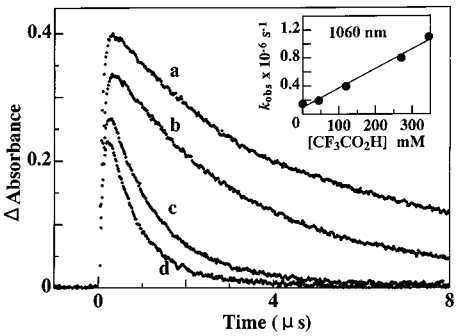

Figure 8. Long-time decay profiles of $C_{60}^{\bullet-}$ at 1060 nm (produced by the electron transfer from TTF to $^3C_{60}$*) in the presence of CF_3CO_2H in Ar-saturated benzonitrile; $[CF_3CO_2H]$ 0.0 (a), 120 (b), 270 (c), and 345 mM (d). Insert shows pseudo-first-order plot.

reaction probably proceeds as shown in Scheme 4. There are two possible routes for the addition process, i.e., (i) initial protonation of $C_{60}^{\bullet-}$ to form $H-C_{60}^{\bullet}$, which then combines with $^{\bullet}SC_6H_4NH_2$ to give the addition product ($H-C_{60}-SC_6H_4-NH_2$),[29a] and (ii) coupling of the thio radical with $C_{60}^{\bullet-}$ to form $C_{60}-SC_6H_4NH_2$, which then undergoes protonation to give $H-C_{60}-SC_6H_4NH_2$.[29b]

Protonation of $C_{60}^{\bullet-}$. To evaluate the rate constant for protonation (k_p), the decay kinetics of $C_{60}^{\bullet-}$ were followed in the presence of strong acids such as CF_3CO_2H, which dissociates into $CF_3CO_2^-$ and H^+ in polar solvents such as benzonitrile. When *p*-ABT (or *o*-ABT) was used as the electron donor, the formation of $C_{60}^{\bullet-}$ was suppressed in the presence of CF_3CO_2H due to protonation of the NH_2 group. To detect the protonation of $C_{60}^{\bullet-}$, we chose tetrathiafulvalene (TTF) as the appropriate electron donor, since it does not react with acid.[10−14] Decay profiles of $C_{60}^{\bullet-}$ that result from the protonation reaction are shown in Figure 8. Upon addition of acid, the decay kinetics of $C_{60}^{\bullet-}$ at 1060 nm change from second-order to first-order kinetics, with the first-order rate constants (k_{obs}) increasing with $[CF_3CO_2H]$. From the pseudo-first-order plot (inset in Figure 8), the k_p value was evaluated to be 3.0×10^6 M^{-1} s^{-1} in benzonitrile.

In Scheme 4, the value of k_{rc} can be assumed to be of similar order as the diffusion controlled limit (10^9 M^{-1} s^{-1}). Thus, the radical coupling/protonation route may be more plausible than the protonation/radical coupling route.

Summary

For photoinduced electron transfer, the amino group is indispensable as a substituent for donation of an electron from thiols, phenols, and disulfides to $^3C_{60}$* in polar solvents. For the photoadduct formation, both the thiol and amino groups are necessary, because deprotonation of $H_2NC_6H_4SH^{+\bullet}$ occurs before the radical addition to $C_{60}^{\bullet-}$. These reaction processes can be followed step by step by the combination of laser flash photolysis and steady-state measurements.

Acknowledgment. The authors express thanks to Mr. K. Furukawa of the Co Irradiation Center in Tohoku University for γ-irradiation. The present work was partly supported by a Grant-in-Aid for priority-area research on "carbon alloys" (No. 10137203) from the Ministry of Education, Science, Sports and Culture.

References and Notes

(1) Sension, R. J.; Szarka, A. Z.; Smith, G. R.; Hochstrasser, R. M. *Chem. Phys. Lett.* **1991**, *185*, 179.

(2) Arbogast, J. W.; Foote, C. S. *J. Am. Chem. Soc.* **1991**, *113*, 8886.

(3) (a) Biczok, L.; Linschitz, H. *Chem. Phys. Lett.* **1992**, *195*, 339. (b) Gupta, N.; Linschitz, H.; Biczok, L. *Fullerene Sci. Technol.* **1997**, *5* (2), 343. (c) Biczok, L.; Gupta, N.; Linschitz, H. *J. Am. Chem. Soc.* **1997**, *119*, 12601.

(4) Arbogast, J. W.; Foote, C. S.; Kao, M. *J. Am. Chem. Soc.* **1992**, *114*, 2277.

(5) Nonell, S.; Arbogast, J. W.; Foote, C. S. *J. Phys. Chem.* **1992**, *96*, 4169.

(6) Osaki, T.; Tai, Y.; Tazawa, M.; Tanemura, S.; Inukawa, K.; Ishiguro, K.; Sawaki, Y.; Saito, Y.; Shinohara, H.; Nagashima, H. *Chem. Lett.* **1993**, 789.

(7) (a) Guldi, D. M.; Hungerbuhler, H.; Janata, E.; Asmus, K.-D. *J. Chem. Soc., Chem. Commun.* **1993**, 84. (b) Guldi, D. M.; Asmus, K.-D. *J. Phys. Chem. A* **1997**, *101*, 1472.

(8) Ghosh, H.; Pal, H.; Sapre, A. V.; Mittal, J. P. *J. Am. Chem. Soc.* **1993**, *115*, 11722.

(9) Sasaki, Y.; Yoshikawa, Y.; Watanabe, A.; Ito, O. *J. Chem. Soc., Faraday Trans.* **1995**, *91* (15), 2287.

(10) Alam, M. M.; Watanabe, A.; Ito, O. *J. Photochem. Photobiol., A* **1997**, *104*, 59.

(11) Alam, M. M.; Watanabe, A.; Ito, O. *Bull. Chem. Soc. Jpn.* **1997**, *70*, 1833.

(12) Nakatsuji, K.; Nakatsuka, M.; Yamochi, H.; Murata, I.; Harada, S.; Kasai, N.; Yamamura, K.; Yamamura, J.; Tanaka, J.; Saito, G.; Enoki, T.; Inokuchi, H. *Bull. Chem. Soc. Jpn.* **1986**, *59*, 207.

(13) Lichtenberger, D. L.; Johnston, R. L.; Hinkelmann, K.; Suzuki, T.; Wudl, F. *J. Am. Chem. Soc.* **1990**, *112*, 3302.

(14) Bryce, M. R. *Chem. Rev.* **1991**, *20*, 355.

(15) (a) Alam, M. M.; Watanabe, A.; Ito, O. *J. Org. Chem.* **1995**, *60*, 3440. (b) Alam, M. M.; Fujitsuka, M.; Watanabe, A.; Ito, O. *J. Phys. Chem. A* **1998**, *102*, 1338.

(16) Watanabe, A.; Ito, O. *J. Phys. Chem.* **1994**, *98*, 7736.

(17) (a) Stewart, J. J. P. *J. Comput. Chem.* **1989**, *10*, 209. (b) Dewar, M. J. S. et al. *J. Am. Chem. Soc.* **1985**, *107*, 3902.

(18) Kajii, Y.; Nakagawa, T.; Suzuki, S.; Achiba, Y.; Obi, K.; Shibuya, K. *Chem. Phys. Lett.* **1991**, *181*, 100.

(19) Sension, R. J.; Phillips, C. M.; Szarka, A. Z.; Romanow, W. J.; Macghie, A. R.; McCauley, J. P.; Smith, A. B., III, Jr.; Hochstrasser, R. M. *J. Phys. Chem.* **1991**, *95*, 6075.

(20) Ebbesen, T.; Tanigaki, K.; Kuroshima, S. *Chem. Phys. Lett.* **1991**, *181*, 501.

(21) Dimitrijievic, N. M.; Kamat, P. V. *J. Phys. Chem.* **1992**, *96*, 4811.

(22) Greaney, M. A.; Gorun, S. M. *J. Phys. Chem.* **1991**, *95*, 7142.

(23) Gasyna, Z.; Andrews, L.; Schatz, P. N. *J. Phys. Chem.* **1992**, *96*, 1525.

(24) (a) Guldi, D. M.; Hungerbuhler, H.; Janata, E.; Asmus, K.-D. *J. Phys. Chem.* **1993**, *97*, 11258. (b) Guldi, D. M.; Hungerbuhler, H.; Asmus, K.-D. *Fullerenes*; Kadish, K. M., Ruoff, R. S., Eds.; The Electrochemical Society Inc.: NJ, 1994; pp 854−864.

(25) Watanabe, A.; Ito, O.; Mochida, K. *Organometallics* **1995**, *14*, 4281.

(26) Arbogast, J. W.; Darmanyan, A. P.; Foote, C. S.; Rubin, Y.; Diederich, F. N.; Alvarez, M. M.; Anz, S. J.; Whetten, R. L. *J. Phys. Chem.* **1991**, *95*, 11.

(27) Steren, C. A.; von Willigen, H.; Biczok, L.; Gupta, N.; Linschitz, H. *J. Phys. Chem.* **1996**, *100*, 8920.

(28) Heath, G. A.; McGrady, J. E.; Martin, R. L. *J. Chem. Soc., Chem. Commun.* **1992**, 1272.

(29) (a) Fukuzumi, S.; Suenobu, T.; Kawamura, S.; Ishida, A.; Takamuku, S.; Mtsumoto, S.; Mikami, K. *Fullerenes*; Kadish, K. M., Ruoff, R. S., Eds.; The Electrochemical Society Inc.: NJ, 1996; Vol. 3, pp 264−275. (b) Mikami, K.; Mtsumoto, S.; Ishida, A.; Takamuku, S.; Suenobu, T.; Fukuzumi, S. *J. Am. Chem. Soc.* **1995**, *117*, 11134.

(30) Ito, O.; Matsuda, M. *J. Am. Chem. Soc.* **1982**, *104*, 568.

(31) (a) Huyser, E. S. In *Advances in Free-Radical Chemistry*; Williams, G. H., Ed.; Logos Press: New York, 1965; Vol. 1, p 77. (b) Ito, O.; Matsuda, M. *J. Am. Chem. Soc.* **1981**, *103*, 5871.

(32) Chatgilialoglu, C.; Asmus, K.-D. *Sulfur-Centered Reactive Intermediates in Chemistry and Biology*; NATO ASI Series A: Life Science Plenum Press: New York, 1990; Vol. 197, pp 155−172.

(33) (a) Ito, O.; Sasaki, Y.; Watanabe, A.; Mochida, K. *Bull. Chem. Soc. Jpn.* **1996**, *69*, 2167. (b) Ito, O.; Sasaki, Y.; Watanabe, A.; Hoffmann, R.; Siedschlag, C.; Mattay, J. *J. Chem. Soc., Perkin Trans. 2* **1997**, 1007.

(34) (a) Hirsch, A. *The Chemistry of the Fullerenes*; Georg Thieme Verlag: Stuttgart, 1994. (b) Hirsch, A.; Lamparth, I.; Karfunkel, H. R. *Angew. Chem.* **1994**, *106*, 453. (c) Isaacs, L.; Haldimann, R. F.; Diederich, F. *Angew. Chem., Int. Ed. Engl.* **1994**, *33*, 2339.